RADIATION RESEARCH **189**, 225–237 (2018)
0033-7587/18 $15.00

DOI: 10.1667/RR14948.1

Synergy Theory in Radiobiology

Dae Woong Ham,[a] Binglin Song,[b] Jian Gao,[a] Julien Yu[a] and Rainer K. Sachs[b,1]

Departments of [a] Statistics and [b] Mathematics, University of California at Berkeley, Berkeley, California

Ham, D. W., Song, B., Gao, J., Yu, J. and Sachs, R. K. Synergy Theory in Radiobiology. *Radiat. Res.* 189, 225–237 (2018).

Customized open-source software is used to characterize, exemplify, compare and critically evaluate mathematical/computational synergy analysis methods currently used in biology, and used or potentially applicable in radiobiology. As examples, we reanalyze some published results on murine Harderian gland tumors and on *in vitro* chromosome aberrations induced by exposure to single-ion radiations that simulate components of the galactic cosmic ray field. Baseline no-synergy/no-antagonism-mixture dose-effect relationships are calculated for corresponding mixed fields. No new experimental results are presented. Synergy analysis of effects due to a mixed radiation field whose components' individual dose-effect relationships are highly curvilinear should not consist of simply comparing to the sum of the components' effects. Such curvilinearity must often be allowed for in current radiobiology, especially when studying possible non-targeted ("bystander") effects. Consequently, many different synergy analysis theories are currently used in biology to replace simple effect additivity. We give evidence that for most synergy experiments and observations, incremental effect additivity is the most appropriate replacement. It has a large domain of applicability, being useful even when pronounced individual dose-effect relationship curvilinearity is a confounding factor. It allows calculation of 95% confidence intervals for baseline mixture dose-effect relationships taking into account parameter correlations; if non-targeted effects are important this gives much tighter intervals than neglecting the correlations. It always obeys two consistency conditions that simple effect additivity usually fails to obey: a "mixture of mixtures principle" and the standard "sham mixture principle". The mixture of mixtures principle is important in radiobiology because even nominally single-ion radiations are usually mixtures when they strike the biological target, due to intervening material. It is not yet clear whether mixing galactic cosmic ray components sometimes leads to statistically significant synergy for animal tumorigenesis. The substantial limitations of synergy theories are sometimes overlooked, and they warrant further study. © 2018 by Radiation Research Society

INTRODUCTION

Ionizing radiation fields are often comprised of mixed rather than just one radiation quality. More generally, agent mixtures, e.g., mixtures of therapeutic drugs or toxins, are important in biology. Dose-effect relationships for effects such as cell killing, gene mutation, chromosome aberrations (CA), cancer relative risk etc. are central in radiobiology. Typically, the main information on mixture components comes from their individual dose-effect relationships (IDERs). There is a need to determine when mixture data indicate synergy, antagonism or neither, and this is usually quantified by comparing an observed mixture dose-effect relationship (MIXDER) with a baseline MIXDER defining the absence of synergy/antagonism.

Researchers in various fields have known for a very long time (*1, 2*) that the ''obvious'' method of comparing mixture effects with simply adding component effects is wrong unless each mixture component IDER is approximately linear-no-threshold (LNT) (*3–8*). A replacement for simple effect additivity is therefore often needed. This article discusses theoretical and computational aspects of the replacements.

Terminology

Several acronyms are used in this article. Table 1 lists the main ones, with those that may be less familiar but often used here indicated in boldface, such as IDER and MIXDER. The table also lists some of the most frequently used mathematical functions. Supplementary Section A1 (http://dx.doi.org/10.1667/RR14948.1.S1) provides more detailed lists.

Mixtures and their Components

A mixed radiation field consists of $N \geq 2$ components. Each component, when acting by itself, has a dose-effect relationship consisting of background plus radiogenic contributions. We define the component's IDER as the

Editor's note. The online version of this article (DOI: 10.1667/RR14948.1) contains supplementary information that is available to all authorized users.

[1] Address for correspondence: Department of Mathematics, MC 3840, Evans Hall, UC Berkeley, Berkeley, CA 94720; email: sachs@math.berkeley.edu.

TABLE 1
List of Acronyms and Functions

Acronym or function	Definition
CA	Chromosome aberration(s).
dE_j/dd_j	The slope of an individual dose-effect relationship (IDER).
$D_j(E_j)$	The compositional inverse function of a monotonic IDER: $D_j[E_j(d_j)] = d_j$.
$d_j = r_j d$	Dose of the jth mixture component as a fraction r_j of total mixture dose d.
$E_j(d_j)$	IDER for the jth component of a mixture.
$E(d)$	IDER.
GCR	Galactic cosmic rays. The mixed radiation field in interplanetary space.
HG	Harderian gland. An organ found in many rodents.
HZE	High-Z and -E (charge and energy) atomic nuclei, almost fully ionized.
$I(d)$	Incremental effect additivity MIXDER and approach.
IDER	Individual dose-effect relationship, for a single agent or single mixture component.
MIXDER	Mixture dose-effect relationship.
L = LET	Linear energy transfer, stopping power, LET_∞.
LNT	Linear-no-threshold. A straight line through the origin (dose = 0, effect = 0).
NTE	Non-targeted effect(s) due to intercellular interactions. ''Bystander'' effect(s).
ODE	Ordinary differential equation.
r_j	Fixed ratio of component dose to total mixture dose, $r_j = d_j/d$, $0 < r_j < 1$.
$S(d)$	Simple effect additivity MIXDER and approach.
TE	Targeted effect(s). Standard radiobiology action due to a direct hit or near miss.
WGE	Whole genome equivalent. For CA scoring with partially painted genomes.

Notes. Several acronyms are used in this article, and the main ones are listed here. Those that may be less familiar but are frequently used in this article are indicated in boldface.

radiogenic contribution. Thus, by definition IDERs are zero when there is no dose above background.

Weaknesses of Simple Effect Additivity

Figure 1 shows examples of why replacements for simple effect additivity are needed when highly curvilinear IDERs are involved. In both panels, while a no-synergy antagonism baseline MIXDER (dashed red curve) should lie approximately halfway between the two IDERs for a 50–50 mixture, it instead actually falls below (panel A) or above (panel B) both IDERs.

More generally, a simple effect additivity baseline MIXDER is always unreasonably large or small, respectively, if all component IDERs are strictly concave or convex, respectively. A very famous concomitant, reviewed in (*4*), is the failure to obey what is called the ''sham mixture principle''. For example, suppose a one-ion beam has dose-effect relationship $E = d^2$. Regard the beam as a 50–50 mixture of two components, each of which happens to have the same IDER, $E = d^2$. Then calculating MIXDER for this sham mixture by simple effect additivity gives $(d/2)^2 + (d/2)^2 = d^2/2$. But of course one cannot cut the beam's toxicity in half by mental gymnastics: the IDERs are curvilinear, so simple-effect additivity should not be used to define absence of synergy/antagonism. Such problems with simple effect additivity are well known in pharmacometrics, toxicology, evolutionary ecology and other fields of biology (*6*). Alternatives are needed to plan and interpret mixture experiments.

The IDERs for Fig. 1A are linear-quadratic (LQ). In the special case that all mixture components are LQ, a biophysically motivated, often used, highly credible replacement for simple effect additivity is the dual radiation action MIXDER (*3*). However, the scope of the dual radiation MIXDER is limited. For example, the main curvilinearity considered in this article will be pronounced concavity at very low doses. Convexity due to quadratic action will not play a major role because we will emphasize high-LET, low-dose radiation. Thus, the dual radiation action MIXDER will not be used.

Many Synergy Theories

In biology, there are now many different synergy theories. Some of the theories are described, reviewed and compared in (*3–18*). Generally, no two of these theories are fully equivalent, though almost all give the same results for a mixture each of whose components' IDERs is LNT. To avoid confusion, which is rife in this area, it is important to characterize carefully the particular theory used (*6*).

This article emphasizes one recently introduced alternative to simple effect additivity: incremental effect additivity (*17*). ''Incremental'' refers to the fact that an ordinary differential equation (ODE) is used. Intuitively speaking, incremental effect additivity deals with slopes; an IDER slope of course defines a linear relationship between a sufficiently small dose increment and the corresponding effect increment (*19*). Thus, by analyzing sufficiently small increments one can circumvent the curvilinearities that plague simple effect additivity estimates. For example, incremental effect additivity always obeys the sham mixture principle. An incremental approach has become practical because computers have become adept at solving non-linear ODE.

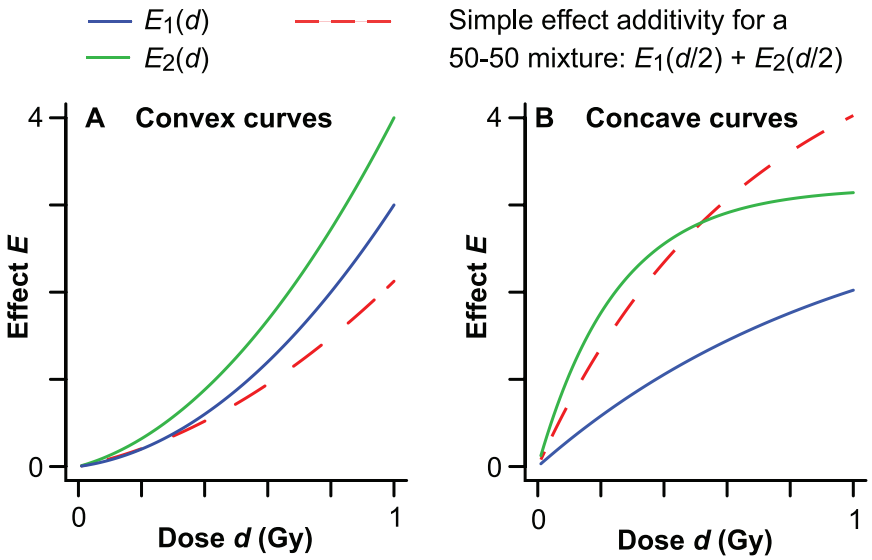

FIG. 1. Simple effect additivity is not appropriate when highly curvilinear IDERs are involved. In panel A the two IDERS have the equations $E = \alpha d + \beta d^2$, with α having dimensions Gy^{-1}, β having dimensions Gy^{-2}, $\alpha_1 = 0.5$, $\beta_1 = 2.5$, $\alpha_2 = 1$ and $\beta_2 = 3$. The second derivative 2β is >0 for both IDERs, which implies the curves are strictly convex. In panel B the two IDERs have equations $A[1 - \exp(-\alpha d)]$ with A dimensionless, $A_1 = 3.2 = A_2$, $\alpha_1 = 1\ Gy^{-1}$ and $\alpha_2 = 4\ Gy^{-1}$, negative second derivatives and therefore strictly concave shapes.

Limitations of Synergy Theories

All known synergy theories have substantial limitations. Because such limitations are sometimes soft-pedaled, we give details on some of the major ones. For example, every published alternative to simple effect additivity requires some restrictions on IDERs that limit its scope. Often monotonic increasing IDERs are explicitly required or implicitly assumed.

Another problem, already mentioned above, is that synergy theory produces only a baseline MIXDER. Mixture component interactions can produce synergy or antagonism, i.e., deviations from the baseline. Mathematical manipulations of IDERs are needed to define synergy but cannot predict it (*10*). If there is significant synergy or antagonism, biophysical insights and multiple mixture experiments or observations, not just mathematical manipulations of IDERs, are needed to characterize mixture effects (*3–5, 20, 21*). A related limitation is that *in silico* synergy analysis becomes less and less important as fundamental biophysical understanding of mixture effects grows (Fig. 2).

Non-Targeted Effects (NTE) and IDER Curvilinearity

At sufficiently small radiation doses and high LETs, only a small fraction of all cell nuclei suffer a direct hit by a radiation track (*22, 23*). Non-targeted effects are then suspected to be important (*24–30*), with cells directly hit by an ion influencing nearby cells through intercellular signaling (*31*). Models of NTE action that are comparatively smooth (i.e., have continuous first and second derivatives) use IDERs that are very curvilinear, specifically very concave, at low doses (*32*). So for small doses and high LETs, replacements for the simple effect additivity synergy theory are needed.

Preview

To illustrate synergy theory, this article emphasizes calculating baseline no-synergy/no-antagonism MIXDERs for recently proposed and for illustrative hypothetical mixture experiments. We will use mixture examples, such as those simulating aspects of the mixed radiation field above low earth orbit, where some of the components are believed to induce NTE at very low doses. Therefore, in view of the comments in the previous sub-section on NTE and IDER curvilinearity, our examples will often compare incremental effect additivity and simple effect additivity MIXDERs.

Supplementary Sections A1–5 (http://dx.doi.org/10.1667/RR14948.1.S1) supplement the specific examples with a broader overview of current synergy analysis, emphasizing mathematical and statistical aspects relevant or potentially relevant to radiobiology. For example, Supplementary Section A5 discusses a ‘‘mixtures of mixtures principle’’ relevant to radiobiological synergy analyses because of the fact, reviewed, e.g., in (*21, 25*), that each individual component of a mixed radiation field is usually itself a mixture due to degradation (e.g., by self-shielding when a mouse twists in such a way that part of its body is in front of the organ of interest) by the time it hits its target.

METHODS

Customized Software

We used the open-source computer language R (*33*), which was initially designed for statistical calculations, and is now rapidly gaining acceptance among modelers (*34*). Our customized programs are available at http://bit.ly/2iVgWbq and at http://bit.ly/2zJDiqL. Readers can freely download, use and modify them to evaluate our conclusions critically.

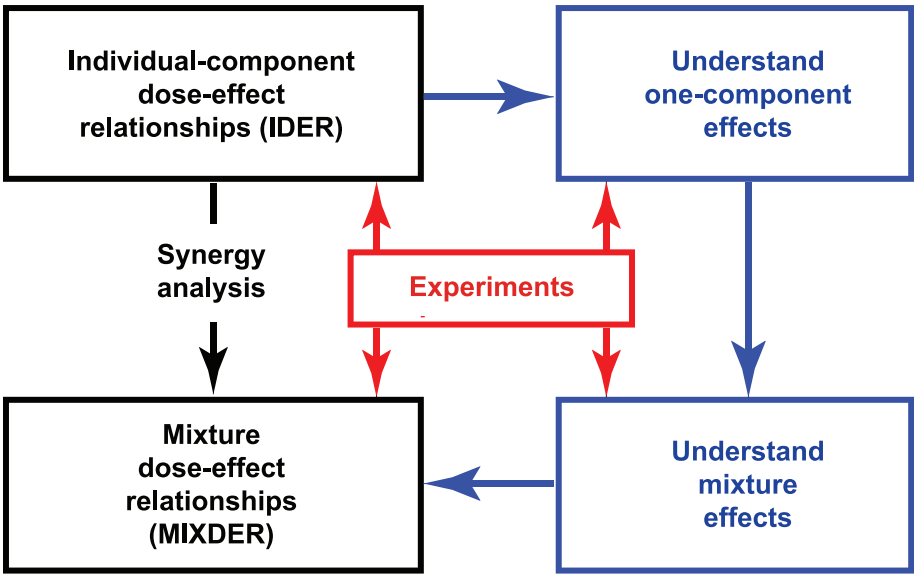

FIG. 2. Investigating mixture effects: a long hard road or a temporary shortcut. Eventually, but almost certainly not soon, synergy analysis of mixed radiation field effects based solely on mathematical manipulations of IDERs (leftmost downward arrow), will be replaced by biophysically-based predictions that incorporate whatever synergy or antagonism actually occurs (blue path). For the time being, optimizing synergy theory, a much simpler, faster and less costly shortcut, is important.

IDERs

Some notation. Mixed N-beam irradiation with dose d_j of component beam j ($j = 1, \ldots, N$) is considered. Component IDERs are denoted as $E_j(d_j)$, or sometimes $E(d)$. Sometimes biophysical parameters such as LET L are used to characterize the different components and replace the label j, e.g., $E(d;L)$ instead of $E_j(d_j)$.

Standard IDERs. We define an IDER $E_j(d_j)$ as "standard" if it obeys the following two restrictions. It has continuous first and second derivatives at all relevant doses including $d = 0$. For example a linear IDER with threshold is not standard because at the threshold point the first derivative is discontinuous and the second derivative is infinite. The second restriction is that $E_j(d_j)$ is monotonically increasing in some half-open dose interval $[0, A_j)$.

Calibrating background and radiogenic effects separately. Synergy is typically considered to be due to interactions among agents. Our mathematical synergy analysis applies to radiogenic effects. In calibrating $E_j(d_j)$ from data, we always use only data at non-zero doses, $E_j(0)$ being 0 by definition. Background, designated by Y_0, is based on the zero-dose data for sham-irradiated controls. Y_0 is needed when calibrating IDERs from data or comparing baseline MIXDERs to data. However, the main synergy calculations involve only IDERs, not background plus radiogenic, effects.

Synergy Theory Calculations

Notation. Consider acute irradiation with a mixed beam of $N \geq 2$ different radiation qualities. The dose proportions r_j that the different qualities contribute to total dose $d = \sum_{j=1}^{N} d_j$ obey the equations:

$$d_j = r_j d; \quad r_j > 0; \quad \sum_{j=1}^{N} r_j = 1. \tag{1}$$

In our subsequent calculations r_j will always, for convenience, be independent of dose. Dose-independent proportions r_j model one typical pattern for irradiation. The assumption of dose-independent proportions does not affect the final results. It implies that any one of the d_j can be considered a control variable on essentially the same footing as the total dose d, since d_j determines d, via $d = d_j/r_j$ with $r_j > 0$, and thereby determines each $d_i = r_i d_j/r_j$. However, we will distinguish between the dose control variables d and d_j versus total mixture effect considered as a control variable. In our analyses effect magnitude is sometimes used to determine d and d_j, instead of being determined by one of them.

After parameter calibration, the IDERs $E_j(d_j)$ of all components will here be known as explicit functions of dose, although in general high-quality numerical approximations are almost equally useful in synergy analyses.

Simple effect additivity $S(d)$. Using the notations specified above, the baseline no-synergy/no-antagonism MIXDER of the simple effect additivity theory, denoted by $S(d)$, is:

$$S(d) = \sum_{j=1}^{N} E_j(d_j). \tag{2}$$

We shall sometimes use $S(d)$ as shorthand to indicate the simple effect additivity approach.

Inverse functions. Inverse functions (sometimes called compositional inverse functions) are needed when using effect, rather than dose, as the independent variable. A familiar radiobiology example of inverse functions occurs when calculating the relative biological effectiveness (RBE) of two different radiations. Inverse functions play a prominent role in various synergy theories. The inverse of a monotonically increasing function undoes the action of the function. For example, for $x > 0$, $\sqrt{x^2} = x$, so the positive square root function is the inverse of the squaring function; note that the inverse of x^2 is not x^{-2}. As another example $\exp[ln(x)] = x$ for $x > 0$, and $ln[\exp(y)] = y$, so the functions exp and ln are inverses of each other.

The equation of incremental effect additivity. When simple effect additivity theory $S(d)$ is inappropriate, an incremental effect additivity baseline MIXDER $I(d)$ has a number of conceptual and practical advantages over other known replacements for $S(d)$. A special case of $I(d)$ was defined and motivated in (*17*) under the following assumptions. Suppose we have a mixture of N components with each component IDER "standard", as defined in the sub-section above, Standard IDERs. It follows that each component IDER has a

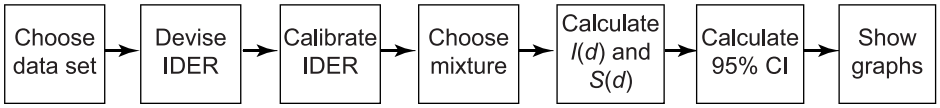

FIG. 3. Flow chart for how we present examples.

compositional inverse function D_j, defined for all sufficiently small non-negative effects E. As discussed in the sub-section above, Inverse functions, this means $D_j(E) = d$ when $E = E(d)$. $I(d)$ was defined as the solution of the following initial value problem for a first order, typically non-linear, ODE:

$$\mathrm{d}I/\mathrm{d}d = \sum_{j=1}^{N} r_j \left[\mathrm{d}E_j/\mathrm{d}d_j\right]_{d_j = D_j(I)}; \quad d = 0 \Leftrightarrow I = 0, \tag{3}$$

with $r_j =$ constant >0 being again the fraction of the total mixture dose contributed by the jth component. Thus, the kth IDER also obeys Eq. (3) but with $r_k = 1$ and all the other $r_j = 0$. Under our assumptions there is a unique, monotonically increasing solution $I(d)$ at least for all sufficiently small non-negative values of d (see Supplementary Section A3.4; http://dx.doi.org/10.1667/RR14948.1.S1).

In Eq. (3), the square bracket with its subscript indicates the following calculations. First, find the slope of the jth IDER curve as a function of individual dose d_j. Then evaluate d_j using the inverse function D_j with the argument of D_j being the effect I already present due to the influence of all the components acting jointly. Using $d_j = D_j(I)$ in Eq. (3) instead of the seemingly more natural $d_j = D_j(E_j)$ is the key assumption made. Using $d_j = D_j(E_j)$ would merely lead back to simple effect additivity $S(d)$, as proven in Supplementary Section A3.4 (http://dx.doi.org/10.1667/RR14948.1.S1).

Equation (3) can be interpreted as follows. As the total mixture dose d increases slightly, every individual component dose d_j has a slight proportional increase, since $\mathrm{d}d_j/\mathrm{d}d = r_j > 0$. Therefore, every mixture component contributes some incremental effect. The size of the incremental effect is determined by the state of the biological target, specifically by the total effect already contributed by all the components collectively (and not by the dose the individual component has already contributed). In this way different components appropriately track changes of slope both in their own IDER and in the other IDERs. Equation (3) is a special case of the general equation of incremental additivity, given in Eq. (20) below, which applies when some mixture components have non-standard IDERs. For the time being we assume all component IDERs for a mixture are standard, as defined in the sub-section, Standard IDERs, and confine attention to Eq. (3).

Computational implementation. Synergy theory is applied using the IDERs with $E_j(0) = 0$, and then the background Y_0 is added back in to the calculated baseline no-synergy/no-antagonism MIXDER for potential comparison to observed mixture results. Computing $I(d)$ for mixtures requires using a one-dimensional root finder within a numerical ODE integrator. Details on these calculations are available on GitHub.

Uncertainties in Mixture Effects

Synergy theory requires not only a way to calculate a baseline MIXDER defining no-synergy/no-antagonism but also a method of estimating uncertainties for the baseline MIXDER from mixture component IDER uncertainties. Taken together, these two elements constitute a default hypothesis useful for statistical significance tests on mixture observations. Without such tests, it is sometimes unclear whether an unexpectedly large or small observed result calls for a follow-up experiment. We used Monte Carlo simulations (*35*) to calculate 95% confidence intervals (CI) for $I(d)$. Because it is known that neglecting correlations between calibrated parameters tends to overestimate how large CI are [internet supplement to (*17*)], we used sampling techniques guided by variance-covariance matrices.

Illustrating Synergy Theory with Examples

We will use two different radiobiology data sets, both of which are for high energy-high charge (HZE) one-ion beams and for LETs greater than 20 keV/μm. One is for chromosome aberrations and the other is for murine Harderian gland (HG) tumorigenesis; both are further described below. Taken together, these can illustrate many aspects of radiobiologically relevant synergy theory. In both cases, we will proceed as follows. For data on one-ion mono-energetic radiations, choose IDERs that depend on several adjustable parameters. Then calibrate the adjustable parameters from the data by non-linear inverse least squares weighted regression. The weights were calculated according to the equations in (*26*) or (*36*), respectively, for the CA and HG data sets. Typical outputs for the calibration step are adjustable parameter values and variance-covariance matrices. Synergy theory calculations are then performed, and the final results are presented in figures illustrating specific aspects of interest. Figure 3 summarizes these steps.

We emphasize that the first 3 steps in Fig. 3 concentrate on aspects needed for the later steps, not on the mechanistic or practical implications of the data. The biophysical and translational aspects of the data have been discussed in the literature. Here we focus instead on synergy calculations and their implications. The CA data set will be used for four graphs, the HG data set for one additional graph. These examples concern situations where there is evidence that NTE are important, so that IDERs that are highly curvilinear at very low doses are needed.

To discuss one additional aspect of synergy theory we devised a purely illustrative IDER without adjustable parameters, thus skipping the first and third panels of Fig. 3 completely. This IDER and its use in mixture calculations are discussed in the sub-section, A Hypothetical Illustrative IDER, below.

Chromosome Aberration Examples

Data. Two recently published studies, (*26, 28*) include data on whole genome equivalent (WGE) simple chromosome aberrations induced by acute *in vitro* exposure, at Brookhaven NASA Space Radiation Laboratory (NSRL), of human cell line 82-6 fibroblasts to the one-ion beams shown in Table 2. Details on the zero-applied dose (sham-irradiated, background, control) data are given in the next sub-section. As for data for non-zero doses, details for each ion, including the number of cells at each dose, are given in (*26*, *28*) and the internet supplement to (*28*). These details are repeated in the open-source scripts freely available on GitHub, as described above in sub-section, Customized Software.

The ions are thus HZE and high LET. The data are for experiments where the only shielding was from matter unavoidably in the beam, with no extra shielding intentionally added. Evidence that at very low doses NTE produce CA in these fibroblasts was given in (*28*).

Similar 82-6 fibroblast experiments at NSRL are ongoing. These sometimes use additional kinds of ions (such as protons), or, importantly for our purposes, ion mixtures. The results have not yet been published and are not considered here in our present article. However, we have aimed at providing a suitable framework for systematic synergy analysis of the ongoing mixture experiments, using information on their component's IDERs from (*26, 28*), and/or from subsequent one-ion experiments.

Small background CA frequency. In synergy calculations, background effects are first subtracted out, as described in the sub-section titled Calibrating Background and Radiogenic Effects Separately. For the HZE experiments in (*26*), there were a total of

TABLE 2
Ion Parameters

	Ion					
Parameter	^{16}O	^{28}Si	^{48}Ti		^{56}Fe	
Z[a]	8	14	22		26	
E/u (MeV)[b]	55	170	600	600	450	300
β^*[c]	0.33	0.53	0.79	0.79	0.74	0.65
L (keV/μm)[d]	75	100	125	175	195	240
Z_{eff}^2/β^{*2}[e]	595	690	770	1075	1245	1585
dmax (Gy)[f]	0.4	1.2	0.6	0.8	0.4	0.8

[a] Z is atomic number.
[b] E/u is kinetic energy per atomic mass unit.
[c] β^* is ion speed relative to the speed of light.
[d] L is *LET*.
[e] Z_{eff} is the effective ion charge, only very slightly less than Z for these high-speed ions.
[f] *dmax* is the maximum dose for that ion in the data set.

7,401 zero-dose control cells in the experiments for five HZE ions, and a total of six whole genome equivalent simple CA scored.[2] Adding in 1,008 control cells for Ti ion experiments with no CA scored [internet supplement to (*28*))] gives an estimate of background effect as $Y_0 = 6/8{,}409 = 7 \cdot 10^{-4}$ per cell. This number is so small that it did not significantly influence any of our results. For example, a sensitivity check, increasing Y_0 by a factor of 2 and recalibrating our models, changed the AIC scores for our model (Supplementary Table A2.3; http://dx.doi.org/10.1667/RR14948.1.S1) by only approximately one part in 10^4 and made no visually perceptible difference to the graphs discussed below.

Preliminary comments. The next step toward synergy analysis was to choose IDERs (Fig. 3). In (*28*) various IDER models, based on modifications of Katz' amorphous track structure approach (*37–40*) were used by Hada, Cucinotta and colleagues to analyze the data; two of their models, reviewed in Supplementary Section A2 (http://dx.doi.org/10.1667/RR14948.1.S1), incorporate both TE and NTE. We modified these two models to obtain our IDERs. To illustrate synergy analysis we needed IDERs that are monotonic increasing and have finite slope at all relevant doses including $d = 0$. Additional criteria we used included the following: keeping the number of adjustable parameters to a minimum; using only adjustable parameters that differ significantly from zero; having Akaike and Bayesian information criteria scores that compare favorably with scores for the two relevant models in (*28*); and otherwise modifying the models in (*28*) as little as possible. We use the same symbols for our adjustable IDER parameters as were used for corresponding parameters in (*28*) in corresponding equations. The correspondences are approximate, not exact.

General properties of our resulting IDERs after calibration are shown in Fig. 4 for one of the ions in Table 2. Corresponding results for the other five ions and detailed comparisons to models in (*28*) are given in Supplementary Section A2 (http://dx.doi.org/10.1667/RR14948.1.S1). The data suggest there is a substantial amount of random noise. At very low doses, where NTE effects putatively dominate, the IDERs rise with a very large but finite slope and have marked curvilinearity, specifically concavity.

Figure 4 A shows qualitative features of the IDERs schematically. To emphasize that there is a finite, smoothly changing slope even near $d = 0$, the steep rise and marked curvilinearity at very low doses have been visually understated. Figures 4B and C are to scale and their curves, actually smooth, incorrectly suggest an infinite slope followed by a kink at $d = 0$.

The steep rise at low doses is inferred indirectly, not observed directly: effects observed at somewhat larger doses (~1 cGy or more) are higher than a LNT model can readily account for. At doses >0.1 Gy, TE putatively dominate and, as Fig. 4 shows, the slope is almost constant, putatively corresponding to high-LET one-track action dominating at doses between 5 and 50 cGy.

Adjustable parameters used. Our IDERs use four adjustable parameters: η_0, η_1, σ_0 and κ. Table 3 shows their units and values after calibration. For example, in the IDERs one term will be of the form $\exp(-\eta_1 L)$. The units of LET L are keV/μm and an exponential must have a dimensionless argument, so η_1 has dimensions μm(keV)$^{-1}$. Table 3 also repeats the value for the background frequency. All four IDER parameters were significantly different from 0 at $p < 0.05$, three at $p < 0.01$ and two at the most stringent level usually considered, $p < 0.001$. These p levels, indicating parsimony, were a pleasant surprise.

IDERs used: equations. Equations (4–9), below, specify our IDERs.

$$E_{total} = Y_0 + E(d; L, Z_{eff}/\beta^*) = Y_0 + E_{TE}(d; L, Z_{eff}/\beta^*) + E_{NTE}(d; L). \quad (4)$$

Here, E_{total} is for background plus radiogenic effect. $E(d;L,Z_{eff}/\beta^*)$ is an IDER, 0 at $d = 0$. E_{TE} and E_{NTE} respectively indicate additive contributions modeling *TE* or *NTE*.

In $E_{TE}(d;L,Z_{eff}/\beta^*)$, the dose dependence is written in terms of ion flux F (i.e., particle tracks per unit area) and a hit number H proportional to F, which are given by:

$$F = 6.242(d/L); \quad H = FA; \quad A = 162\,\mu\text{m}^2. \quad (5)$$

Here, the factor 6.242 applies when areas are given in μm^2 and dose is given in Gy. The value for A was, as described in (*26, 28*), determined by measurements of the beam-perpendicular cross-sectional area of 82-6 fibroblast nuclei. H is the total number of ion track cores that intersect an 82-6 fibroblast nucleus at dose d. Our version of the TE contribution is

$$E_{TE}(d; L, Z_{eff}/\beta^*) = \sigma F[1 - \exp(-H)], \quad (6)$$

where the dose-independent quantity σ is, using the notation of Tables 2 and 3,

$$\sigma = \sigma_0 P + \frac{\alpha_\gamma L}{6.242}(1 - P); \quad P = \left[1 - \exp\left(-\frac{Z_{eff}^2}{\kappa\beta^{*2}}\right)\right]^2. \quad (7)$$

In Eq. (7), we chose the parameter m in the corresponding equation in (*28*) as $m = 2$ on the biophysical grounds that it takes two DNA double-strand breaks to make one simple CA; α_γ is the linear coefficient of the LQ fit to the gamma-ray dose-effect relationship for WGE simple CA per cell. A separate calculation in (*26, 28*) gave $\alpha_\gamma = 0.041 \pm 0.0051$ Gy^{-1}, and here we use this value throughout. Table 3 gives the values of σ_o, and κ. For $\kappa > 0$, $1 > P > 0$.

In Eq. (4), combining Eqs. (5–7) specifies the TE term $E_{TE}(d;L)$ so we only need to specify the NTE contribution to complete the characterization of our IDERs, as follows:

$$E_{NTE}(d; L) = \eta(L)[1 - \exp(-d/d_0)]. \quad (8)$$

Here, much as in (*28*),

$$\eta(L) = \eta_0 L \exp(-\eta_1 L) \quad (9)$$

specifies an LET-dependent saturation level for NTE at doses larger than 1 mGy. The saturation level rises linearly for small LET, reaches a maximum at $L = 1/\eta_1$, and then decreases. For the average value of the adjustable parameter η_1 in Table 3, the maximum occurs at approximately at $L = 110$ keV/μm.

In Eq. (8) d_0 is a nominal, very small dose. The data considered are not informative about any details at very low doses <1 mGy. They do suggest NTE that lead to a large average positive slope at very low doses, whose cumulative influence builds up a CA frequency E_{NTE} sufficiently large to be detectable above background and noise at

[2] Personal communication (M. Hada).

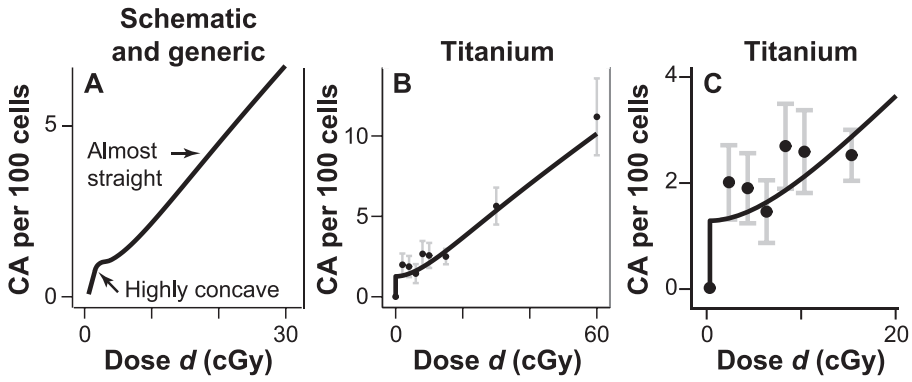

FIG. 4. IDER shape. The vertical axis represents WGE simple chromosome aberrations per 100 cells.

doses ≥ 0.01 Gy. To take into account NTE dose dependence in a way consistent with the concavity found in mechanistic models for NTE for other end points (*32*) we used the factor $[1 - \exp(-d/d_0)]$ and used $d_0 = 10^{-5}$ Gy. Numerical explorations show that the final results are insensitive to d_0 as long as $d_0 \ll 10$ mGy.

Summary of IDER equations. Rearranging Eqs. (4–9) to show more concisely the dependence on all four adjustable parameters (i.e., η_0, η_1, σ_0 and κ), our IDERs $E(d)$ are:

$$E(d) = \eta_0 L \exp(-\eta_1 L)[1 - \exp(-d/d_0)] + [\sigma_0 P + \alpha_\gamma L(1-P)/6.242]F[1 - \exp(-H)], \quad (10)$$

where $\alpha_\gamma = 0.041 \pm 0.0051$ Gy^{-1}, $d_0 = 10^{-5}$ Gy, and

$$P = [1 - \exp(-\kappa^{-1} Z_{eff}^2/\beta^{*2}]^2. \quad (11)$$

The biophysical parameters such as LET L are those in Table 2. In Eq. (10), the first term in the sum is for NTE; the second term is for TE. As shown in Eq. (5), F is the particle flux, proportional to d/L, and hit number H is proportional to F. Thus, when H becomes so large that $\exp(-H)$ is negligible, the TE term has constant slope (Fig. 4).

IDER calibration. The IDERs were calibrated by using non-linear least squares inverse variance weighted regression with the Levenberg-Marquand algorithm to determine the four adjustable parameters from combined data of all six ions at all non-zero doses. The auxiliary parameter α_γ and the background value Y_0 were held fixed at their central values during the calibration. The results for the four adjustable parameters were shown above, in Table 3.

The regression also determined a variance-covariance matrix, shown in Supplementary Table A2.2 (http://dx.doi.org/10.1667/RR14948.1.S1), which we used during synergy analyses in calculating 95% CI for the baseline incremental effect additivity MIXDER $I(d)$. The variance-covariance matrix in turn determined a parameter correlation matrix, shown in Table 4.

An Example Using Murine Harderian Gland (HG) Tumorigenesis Data

Our second example uses a well-known data set. It further illustrates marked IDER curvilinearity. It will again be presented in the order indicated by Fig. 3, starting with IDERs, adjustable parameters and calibration.

Accumulating data. Many rodents have Harderian glands, which comprise epithelial tissue. An extensive set of experimental observations is available on the fraction of female B6CF1/Anl mice that develop at least one radiogenic HG tumor after exposure at various doses to various one-ion HZE beams (*22, 27, 36, 41, 42*). This fraction, the tumor prevalence, is by definition ≤ 1. The HZE ions' parameter ranges are: atomic charge $8 \leq Z \leq 57$; approximate LET $20 \leq L$ (keV/μm) ≤ 950; approximate speed relative to speed of light $0.61 \leq \beta^* \leq 0.81$. All the relevant data in the references are reviewed in customized open-source software freely downloadable from GitHub. Additional data in the same data set, on fast, low-LET protons and alpha particles, will be discussed in the sub-section titled A Hypothetical Illustrative IDER, below. Unpublished data from ongoing experiments include other ions plus some mixed-beam exposures; these as yet unpublished data will not be used in this article.

Adjustable parameters used. Our HZE IDERs use three adjustable parameters: a_1, a_2, and η (Table 5). As in Table 3, we also show the parameter values after they have been calibrated and the value for the background frequency. The background frequency was taken from recent modeling of the same data (*27, 30*) without further calculations on our part, as the emphasis here will again be on using IDERs in synergy analyses rather than biophysically interpreting IDERs.

Thus, all three IDER parameters were significantly different from 0 ($p <$ 1e–5). The most recent published analysis of the same data (*30*) used NTE IDER with four adjustable parameters, three having p values $<10^{-4}$, but one having $p = 0.4$, signaling a possible parsimony problem.

IDERs used. The IDERs we use here for the HZE data modify some of the tumor prevalence models in (*27*) and (*30*); they are NTE

TABLE 3
Calibrated Parameters

	Units	Value	±[b]	p	Comments
Y_0	Dimensionless	7.0e–5[a]	NA	NA	Background. See sub-section titled Small Background CA Frequency
η_0	Dimensionless	2.5e–4	4.60e–5	2.0e–06	Both parameters help specify how NTE magnitude depends on LET L
η_1	μm(keV)$^{-1}$	9.0e–3	1.61e–3	1.1e–6	
σ_0	μm^2	5.96	1.96	3.8e–3	Both parameters help specify TE slope as a function of d, L and Z_{eff}^2/β^{*2}
κ	Dimensionless	695	263	1.1e–2	

[a] Powers of 10 are indicated by "e", for example, 3.5e–3 = 0.0035.
[b] Standard errors are indicated by ±.

TABLE 4
Pairwise Correlations

	η_0	η_1	σ_0	κ
η_0	1	0.96	0.43	0.41
η_1	0.96	1	0.44	0.39
σ_0	0.43	0.44	1	0.96
κ	0.41	0.39	0.96	1

Notes. In this case, all correlations are >0. An intuitive argument for the strong positive correlation between η_0 and η_1 is given in Supplementary Section A2, below Table A2.2 (http://dx.doi.org/10.1667/RR14948.1.S1).

models, i.e., assume both TE and NTE are significant. For all doses, they are less than 1, the maximum possible value, since prevalence refers to animals with at least one tumor.

The starting point for our models is a very useful hazard function equation suggested by Cucinotta and coworkers, e.g., (*30*):

$$E(d) = 1 - \exp[-H(d)] \tag{12}$$

Here $E(d)$ is the IDER and $H(d)$ is a non-negative hazard function, which we shall use to define $E(d)$. Equation (12) is an important improvement over earlier models of the HZE HG data because it incorporates the limitation that $E(d) \leq 1$ without needing to add any extra adjustable parameters. Specifically, we shall use hazard functions which are standard IDERs, as defined in the sub-section, Standard IDERs. Then $E(d)$ in Eq. (12) is automatically also standard.

However, our HZE models do not adopt the Katz type approach of (*30*). We found HZE models with fewer adjustable parameters and improved p values. When applied to NTE models, the approach in (*30*) becomes more difficult to motivate, e.g., with regards to effects of delta rays on NTE and the way in which cell killing terms appear in the equations.

Specifically, we used for H an LET-dependent TE term linear-no-threshold in dose that involves two of the adjustable parameters in Table 5. We added an LET-independent NTE term involving our third adjustable parameter, η, to get the following equation:

$$H(d;L) = a_1 L \exp[-a_2 L]d + \eta[1 - \exp(-d/d_0]. \tag{13}$$

In this equation, d_0 is again a nominal, very small dose having all of the properties given in the paragraph below Eqs. (8) and (9). In particular, all our final results are independent of d_0 provided $d_0 < 10^{-5}$ Gy.

After calibration, our IDERs were considered applicable to all heavy ions in the Z, LET and energy ranges covered by the data, i.e., applicable even to one-ion beams not in the data set. The relevant ranges were $8 \leq Z \leq 43$; $25 \leq L$ (keV/μm) ≤ 950; and $360 \leq E/u$ (MeV) $\leq 1{,}000$.

A Hypothetical Illustrative IDER

We define a ''toy'' IDER as follows:

$$E_{\text{toy}}(d) = M[1 - \exp(-\lambda d)], \quad \text{where } M = 0.28 \text{ and } \lambda = 0.78 \text{ Gy}^{-1}. \tag{14}$$

Here, M is the limiting value at large doses and $M\lambda$ is the slope at $d = 0$. The shape of E_{toy} is somewhat similar to data on fast, low-LET protons and alpha particles in the murine HG tumorigenesis set (*22, 27, 30, 36, 42*). However, the parameters M and λ are quite wrong for actual data in this data set; they are instead chosen to help illustrate one further aspect of synergy analysis; thus we use the label ''toy''. The prevalence limit $M < 1$ means that synergy analyses of a mixed beam containing both HZE ions and fast light ions encounters a difficulty that also arises for some other data sets. We now illustrate the difficulty and how it can be solved.

The slope function dE_{toy}/dd can be expressed explicitly as a function of E_{toy} without using an inverse function in an intermediate step, thereby simplifying the next few equations and allowing them to be an atypically simple illustration of an important general point. The slope is calculated as

$$dE_{\text{toy}}/dd = \lambda M \exp(-\lambda d) = \lambda M\left[1 - \left(E_{\text{toy}}/M\right)\right] = \lambda\left(M - E_{\text{toy}}\right). \tag{15}$$

Thus, Eq. (14) implies:

$$dE_{\text{toy}}/dd = \lambda\left(M - E_{\text{toy}}\right) \tag{16A}$$

and

$$E_{\text{toy}}(d = 0) = 0. \tag{16B}$$

Conversely, Eq. (16) is an ODE initial value problem that has a unique solution. Integrating Eq. (16A) implies that for $E_{\text{toy}} < M$ there is a constant of integration such that

$$-\lambda d = \ln\left(M - E_{\text{toy}}\right) + constant. \tag{17}$$

The initial value, Eq. (16B), then implies the integration constant is –ln(M) and using the fact that exp and *ln* are inverses of each other leads directly back to Eq. (14).Thus, as far as IDERs are concerned, Eqs. (14) and (16) are completely equivalent.

However, for analyzing a mixture of a toy ion with an HZE ion, using Eq. (16) has a surprising advantage. What we need for calculating a baseline MIXDER with the equation of incremental effect additivity, Eq. (3), is not $E_{\text{toy}}(d)$ but the slope dE_{toy}/dd as a function of E_{toy}; replacing E_{toy} by the total effect, say I, due to all the mixture components, we then get the contribution of $E_{\text{toy}}(d)$ to the mixture slope. Thus, if r is the fraction of mixture dose supplied by the toy beam, we can use $r\lambda(M - I)$ as the slope contribution, even at doses so large that the HZE components in the mixture have driven I above M and the toy contribution to the MIXDER slope is negative. In other words, with E_1 denoting the HZE IDER, we can replace Eq. (3) by

$$dI/dd = r_1[dE_1/dd_1]_{d_1 = D_1(I)} + r_2\lambda(M - I); \quad d = 0 \Leftrightarrow I = 0. \tag{18}$$

One intuitive motivation behind Eq. (18) is that, as discussed in motivating Eq. (3), effect I is a system variable, a property of the biological target, rather than being, like d, merely externally imposed. So $I(d)$ can supply information, in this case $r_2\lambda(M - I)$, which can help determine its own incremental changes.

TABLE 5
Calibrated Parameters

	Units	Value[a]	p	Comments
Y_0	Dimensionless	2.7e–2	NA	Background
a_1	μm (keV)$^{-1}$	8.0e–3 ± 1.0e–3[a]	3e–8	Both parameters help specify how TE slope depends on LET L
a_2	μm (keV)$^{-1}$	3.4e–5 ± 4.0e–6	7e–9	
η	Dimensionless	5.0e–2 ± 1.4e–2	2e–6	NTE height

[a] Powers of 10 are indicated by ''e'', for example 2.7e–2 = 0.027. Standard errors are indicated by ±.

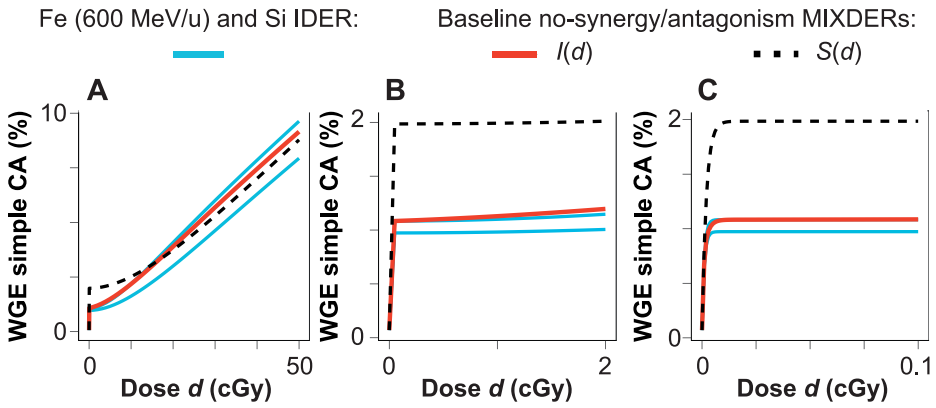

FIG. 5. Synergy analysis for a Si-Fe mixed beam. Shown here are baseline curves (black dashed and red solid) for a mixture of two beams characterized in Table 2: Si and Fe (600 MeV/u) with proportions $r_1 = 0.5 = r_2$. Blue lines show the IDERs that would result if the entire dose were contributed by one of the ion beams instead of being split 50-50. The higher blue curve [hidden behind $I(d)$ in panel C] is for Si. Panel A shows the overall curves up to mixture dose 0.5 Gy. Panels B and C zoom in on smaller doses, with panel C showing details about the mathematical model at doses too small for CA data to be available.

RESULTS FOR MIXTURES

In the following two sub-sections, each example has a data set, IDERs and mixtures (Fig. 3); the mixtures are specified by their components and the components' fraction $r_j d$ of the total mixture dose d. The main results are presented as IDER and baseline MIXDER graphs.

Chromosome Aberrations

Synergy analyses for two-ion and six-ion mixtures: average parameter values. We chose a CA data set and IDERs with four adjustable parameters, and calibrated the IDERs using inverse variance weighted non-linear least squares regression (see sub-section above in Materials and Methods, Chromosome Aberration Examples). The outputs needed for synergy analyses (see Synergy Theory Calculations sub-section, above) were the average values of the adjustable parameters, their variance covariance matrix and the calibrated IDERs. For the moment, we use only the average values shown in Table 3. Uncertainties in MIXDERs are discussed further in the next sub-section.

The only IDERs (or data) for this data set are for primary beams (upstream of any incidental matter in front of the biological target) consisting of a single HZE ion with $Z \geq 8$, so our mixture examples perforce involve only such HZE components. Such mixtures are in any case more interesting than mixtures where most of the dose in the primary beam is contributed by low-LET protons and alpha particles. The HZE part of the galactic cosmic ray (GCR) spectrum has caused much concern regarding astronaut exposures during prolonged periods above low earth orbit [reviewed, e.g., (*27*)], and synergy between specific HZE components would compound these concerns.

Figure 5 shows, for a 50-50 Si-Fe mixture, prototypical results contrasting our preferred no-synergy/no-antagonism baseline MIXDER $I(d)$ with simple effect additivity $S(d)$. As shown in Fig. 5B and C, the NTE part of $S(d)$, which dominates the MIXDER at very low doses, shows saturation at approximately the sum of the two IDER NTE contributions, rather than their average. This is merely the same artificial result shown in Fig. 1B: $S(d)$ tends to be an unrealistic overestimate because all mixture components are highly concave at very low doses: to our knowledge, there are no known mechanistic reasons that NTE effects in a mixture should saturate at effect higher than the height of the NTE part of either component acting by itself. In contrast, the NTE part of $I(d)$ saturates at approximately the larger of the two, a more reasonable result.

Details of the calculations that produced Fig. 5 are encapsulated in the customized open-source programs that can be freely downloaded from GitHub.

The choice $r_1 = 0.5 = r_2$ in the mixture of Fig. 5 was arbitrary. If one wanted to check experimentally whether mixing the two beams ever leads to statistically significant synergy or antagonism, one would have to calculate a few more cases, such as $r_1 = 0.2$, $r_2 = 0.8$ and $r_1 = 0.8$, $r_2 = 0.2$. When we set out to give examples involving $N > 2$ ions, we were unpleasantly surprised to find that, due to the many possible choices of the r_j, the number of possible examples grows very rapidly as N increases. Worse, there is no systematic way to choose any particular example. Thus the example given next is not chosen in any systematic way, and apparently could not be chosen systematically without giving a very large number of examples.

Figure 6 shows another example of a mixture. It illustrates the fact that $S(d)$ for a mixture of many ions, which individually can produce significant NTE, gives an unreasonable baseline MIXDER even at doses large enough for data to be available. In Fig. 6 it specifies that, at low doses, effects much larger than any component would produce if acting by itself with the total mixture dose, are ostensibly not synergistic. Calculations (not shown) indicate

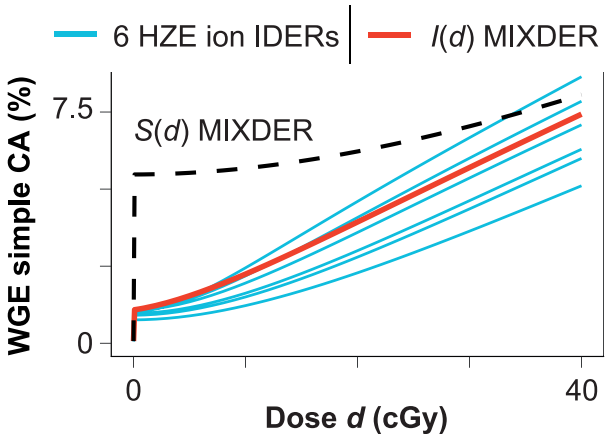

FIG. 6. A multi-ion mixture. Shown here are results for a mixture of all six ions in Table 2, with each contributing one-sixth of the total dose d. The blue lines show the six component IDERs. The IDER curve heights are in reverse order as the LETs; for example, the highest blue curve is for oxygen ions with LET 75 keV/μm while the lowest blue curve is for Fe with energy 300 MeV/u and LET 240 keV/μm. It is evident here that the incremental effect additivity baseline no-synergy/antagonism dose-effect relationship $I(d)$ is similar to the average of the six components but the simple effect additivity baseline $S(d)$ is not.

that if a mixture consists of many more than six HZE ions, the discrepancy at low doses becomes even larger, with $S(d)$ specifying absurdly high effects as defining absence of synergy. In contrast, $I(d)$, as in Fig. 5, specifies saturation near the top of individual component saturation heights and tends to remain nested within the component IDERs.

Synergy analyses for two-ion and six-ion mixtures: 95% CI for I(d). Our calculations include finding 95% CI for $I(d)$. We used Monte Carlo simulations to calculate 95% CI for the incremental effect additivity baseline no-synergy/no-antagonism MIXDER of the two-ion mixture of Fig. 5, taking into account parameter correlations. We had to make *ad hoc* adjustments for cases where κ was not >0. This occurred in approximately two out of 1,000 samples and did not affect the CI significantly. Details are again encapsulated in the customized open-source codes that can be downloaded from GitHub.

We also calculated 95% CI for the six-ion mixture of Fig. 6. To estimate how much neglecting parameter correlations overestimates the 95% CI, we compared two alternative calculations. Figure 8 shows the results. Figure 8A takes parameter correlations into account appropriately and Fig. 8B neglects them. At $d = 40$ cGy, Fig. 8B overestimates the 95% CI by a factor of ~3.07. Such differences can result in a mixture measurement, e.g., the hypothetical black point, which establishes statistically significant synergy (Fig. 8A), being misinterpreted as merely indicative (Fig. 8B). Moreover, NASA guidelines for astronaut exposures heavily emphasize 95% CI [reviewed in (*43*)], so overestimates of CI width can have major policy implications. Thus, taking parameter correlations into account, though often neglected, is important when interpreting mixture experiments.

Summary. We used a CA model that incorporates both TE and NTE effects to illustrate various aspects of mathematical synergy analyses. Assuming non-targeted effects are important, $I(d)$ gives a markedly different, more reasonable, no-synergy/no-antagonism baseline than does $S(d)$ when mixtures of many HZE are considered.

There is a bewildering number of potentially inequivalent mixtures whenever more than a few ions are involved. As yet unpublished data on ongoing experiments will be a test of our IDERs, and will also provide some mixture data to compare with $I(d)$.

HZE Murine Harderian Gland (HG) Results for Incremental Effect Additivity I(d)

For the data set on murine HG prevalence after single-ion HZE irradiation (sub-section titled An Example Using Murine Harderian Gland Tumorigenesis Data) we chose IDERs with three adjustable parameters, and again calibrated the IDERs using inverse variance weighted non-linear least squares regression for all ions at the same time. We graphed MIXDER results using average values for the adjustable parameters: 95% CI for $I(d)$ are sufficiently exemplified in Figs. 7 and 8.

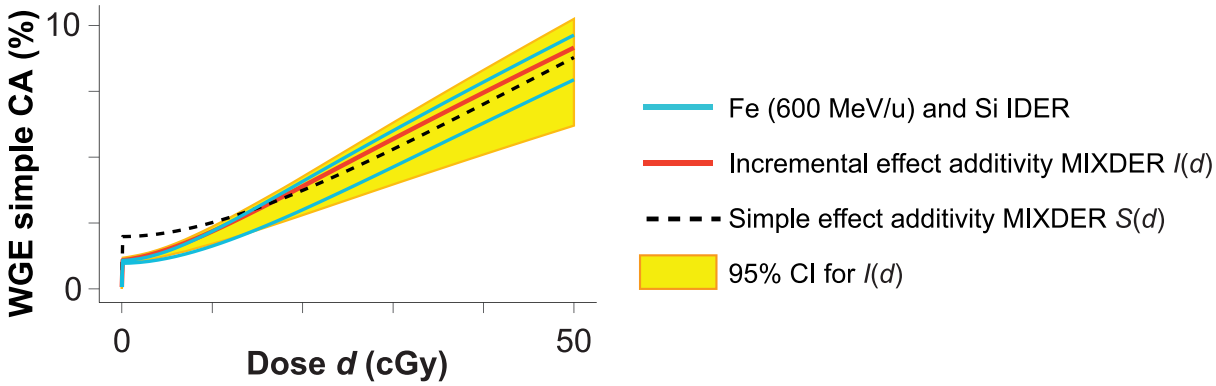

FIG. 7. Confidence interval of 95% in the two-ion mixture. As shown here, for a 50–50 mixture of two HZE radiations the two baseline no-synergy/no-antagonism dose-effect relationships have statistically significant differences only for doses less than approximately 0.05 Gy.

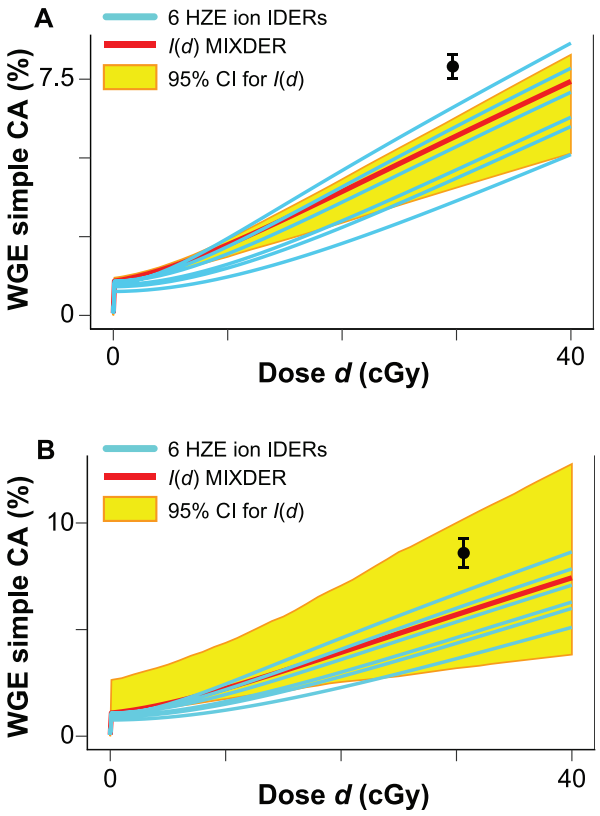

FIG. 8. Confidence interval for $I(d)$. Panels A and B are identical apart from the width of the 95% CI; other visual differences are due only to the difference in the vertical scale. Panel A shows the calculated 95% CI if parameter correlations are taken into account appropriately. Panel B shows calculated 95% CI if the correlations are unrealistically neglected. The black circle with error bars shows a possible data point in a mixture experiment; the point is outside the yellow ribbon in panel A but the same point is inside the yellow ribbon in panel B.

Figure 9 shows an example where simple effect additivity $S(d)$ again unrealistically specifies that a mixture effect larger than that of any component defines absence of synergy and antagonism. Similar calculations show that if more than approximately 20 HZE ions are involved, $S(d)$ makes the impossible claim that absence of synergy or antagonism at 0.5 Gy means the fraction of mice that have at least one tumor is greater than 1. In contrast, $I(d)$ in Fig. 9 is close to the average of the four IDERs at all doses larger than the nominal value of 10^{-5} Gy.

The Advantage of Generalizing the Equation of Incremental Effect Additivity

An example that illustrates Eq. (18) is given in Fig. 10. In each panel the upper blue curve is the IDER for a HZE mixture component that has LET 195 keV/μm. The lower blue curve is the toy IDER. Results for mixtures with two different dose-proportions are shown in the two panels. Equation (18) was used to calculate baseline incremental effect additivity MIXDERs (red curves). As can be proven by using the qualitative theory of ODE (*44*), MIXDERs

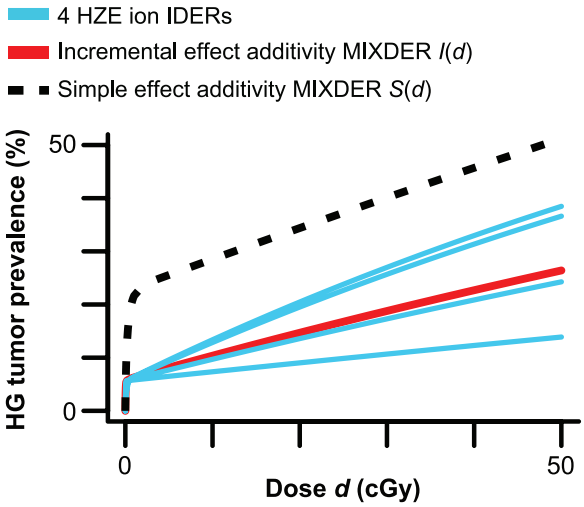

FIG. 9. A four-ion mixture. The figure shows results for ions of respective LETs (from bottom to top): L = 25, 70, 190 and 250 keV/μm. For HG prevalence (unlike WGE simple CA) higher LETs are more damaging. Each ion contributes one-fourth of the total mixture dose d. Blue lines are again the IDERs that would result if one of the ions contributed the entire dose d.

level off at an effect between M and 1 where the tendency of the light ions to pull the MIXDERs down to M just balances the tendency of the HZE component to pull them up to 1.

Equations (3) and (18) give identical curves as long as the baseline MIXDER effect is less than M. The key point is that when the baseline MIXDER effect calculated by Eq. (18) reaches M (red dots) the incremental effect additivity Eq. (3) contains an undefined inverse function for the light ion so it cannot be used to calculate MIXDERs beyond the corresponding doses. This difficulty is rather similar to, though not the same as, the well-known problems [reviewed in (*45*)] that occur in attempts to compute RBEs when a high-LET radiation can produce effects larger than any effect the low-LET reference radiation can produce. Equation (18) solves this problem.

An alternative method of going beyond the cutoff point, setting the contribution of the problematic IDER to $I(d)$ slope equal to zero when $I(d)$ exceeds M, was used in (*17*) but should now be considered obsolete, for reasons discussed in Supplementary Section A5, especially in A5.3 (http://dx.doi.org/10.1667/RR14948.1.S1).

In Fig. 10A and B, cutoff doses are approximately 1.2 Gy and <0.5 Gy, respectively. Typical low-dose NASA mixture experiments do not go as high as 1.2 Gy, but a cutoff at <0.5 Gy would be an unnecessarily strong limitation.

The general equation of incremental effect additivity. Generalizing the results of the previous sub-section, consider IDERs given by

$$dE/dd = F(E); \quad E = 0 \text{ when } d = 0, \tag{19}$$

with the slope function $F(E)$ sufficiently well behaved that there is one and only one solution for all sufficiently small non-negative doses. Consider a mixture consisting of $N \geq 0$ agents whose IDERs are in the form $E_j(d_j)$ together with K

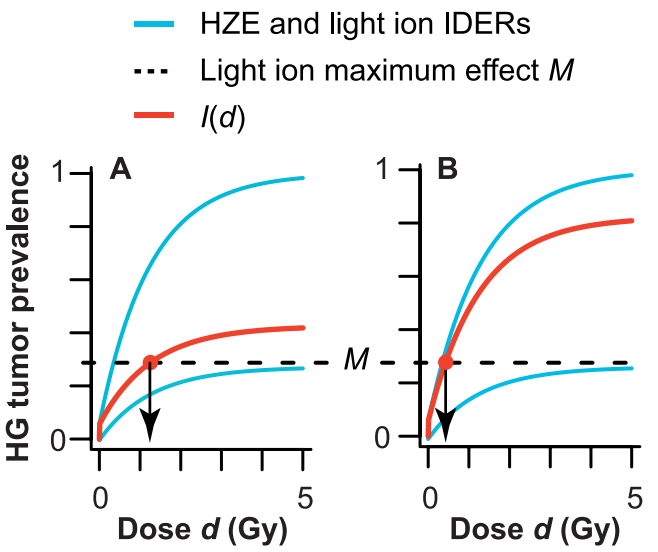

FIG. 10. Mixtures of an HZE ion and a toy Ion. In panel A, the toy radiation contributes $r_1 = 80\%$ of the mixture dose; in panel B, it contributes only $r_1 = 25\%$. $I(d)$ given by Eq. (18) is well defined even for effects greater than M. The cutoff doses corresponding to M are shown by the downward arrows. At dose fraction 80% the toy beam pulls the MIXDER down close to M at large doses. At dose fraction 25% it can only pull it down to somewhat less than 1.

≥ 0 agents whose IDERs are defined by Eq. (19), where $N + K \geq 2$. Let $r_1, r_2, \ldots, r_{N+K}$ be the corresponding proportions. Then the general equation of incremental effect additivity for $I(d)$ is:

$$dI/dd = \sum_{j=1}^{N} r_j \left[dE_j/dd_j\right]_{d_j = D_j(I)} + \sum_{j=N+1}^{N+K} r_j F_j(I); \quad d = 0 \Leftrightarrow I = 0. \tag{20}$$

Supplementary Section A5 analyzes the mathematical properties of this equation in detail and, importantly, shows that it is often applicable even when the restriction that all IDERs be monotonic in the same direction does not hold.

Summary of Results

To illustrate the aspects of synergy theory likely to be most important in radiobiology we gave results exemplifying the following: the importance of having high-quality IDERs available; the use of alternatives, such as incremental effect additivity $I(d)$, to simple effect additivity $S(d)$ when IDER curvilinearity requires an alternative; calculation of baseline MIXDER 95% CI taking into account correlations between IDER adjustable parameters; and the extraordinarily rapid increase in the number of possible mixtures needed to determine synergy patterns for N-component mixtures as N increases.

DISCUSSION

Synergy Theory

For the foreseeable future radiobiologists studying mixed radiation field effects will almost inevitably emphasize possible synergy and antagonism among the different radiation qualities in the mixture. Therefore, trying to find a systematic quantification of synergy, general enough to cover most cases of radiobiological interest and precise enough to enable credible estimates of statistical significance when synergy is indicated by a mixture experiment, it is not easy.

One main problem is the following. The common belief that synergy can always be defined as an effect greater than the simple effect additivity baseline MIXDER $S(d)$ is wrong. $S(d)$ can almost always be calculated, but in some important cases is clearly inappropriate. There are a number of published alternatives that seem appropriate whenever they can be calculated, but are not well defined unless all IDERs in a mixture are monotonic in the same direction. The monotonicity requirement unduly restricts their scope.

Among the alternatives to $S(d)$, the incremental effect additivity baseline MIXDER $I(d)$ seems preferable. Here, we have illustrated it with detailed examples of mixtures of ions in the GCR spectrum, since more experimental information on such mixtures will soon become available.

Summary

Synergy theory will continue to be used to plan experiments involving mixed radiation fields and to interpret the results of such experiments. It can and should include calculations that give $I(d)$ confidence intervals based on variance-covariance matrices.

If non-targeted effects are important, simple effect additivity no-synergy/no-antagonism baseline MIXDERs should be ignored or used only cautiously.

Incremental effect additivity theory is, in our opinion, the preferred replacement for simple effect additivity theory.

With individual dose-effect relationships for components of a mixture all monotonically increasing, there are many other synergy theories that have been developed over many years in many different fields of biology to supplement or replace simple effect additivity.

In any case, all synergy theories have more limitations than has been generally realized.

It is unclear whether mixing GCR components ever leads to statistically significant synergy for animal tumorigenesis. Future mixture experiments will help clarify this question.

ACKNOWLEDGMENTS

This work was supported by NASA (grant no. NNJ16HP221 to RKS) and the UC Berkeley undergraduate research apprenticeship program (URAP; to DWH, BS, JG and JY). We are grateful to Drs. E. A. Blakely, P. Y. Chang and J. H. Mao for useful discussions. We thank Drs. F. A. Cucinotta and M. Hada for clarifying some details of the data sets.

Received: September 21, 2017; accepted: November 14, 2017; published online: December 29, 2017

REFERENCES

1. Fraser TR. Lecture on the antagonism between the actions of active substances. Br Med J 1872; 2:485–7.
2. Loewe S, Muischnek H. Ueber Kombinationswirkungen. I. Mitteilung Hilfsmittel der Fragestellung. Archiv Experimentelle Pathologie Pharmakologie 1926; 114:313–26.
3. Zaider M, Rossi HH. The synergistic effects of different radiations. Radiat Res 1980; 83:732–9.
4. Berenbaum MC. What is synergy? Pharmacol Rev 1989; 41:93–141.
5. Geary N. Understanding synergy. Am J Physiol Endocrinol Metab 2013; 304:E237–53.
6. Foucquier J, Guedj M. Analysis of drug combinations: current methodological landscape. Pharmacol Res Perspect 2015; 3:e00149.
7. Piggott JJ, Townsend CR, Matthaei CD. Reconceptualizing synergism and antagonism among multiple stressors. Ecology and Evolution 2015; 5:1538–47.
8. Tang J, Wennerberg K, Aittokallio T. What is synergy? The Saariselka agreement revisited. Front Pharmacol 2015; 6:181.
9. Zaider M. Concepts for describing the interaction of two agents. Radiat Res 1990; 123:257–62.
10. Lam GK. A general formulation of the concept of independent action for the combined effects of agents. Bull Math Biol 1994; 56:959–80.
11. Lorenzo JI, Sanchez-Marin P. Comments on ''Isobolographic analysis for combinations of a full and partial agonist: curved isoboles''. J Pharmacol Exp Ther 2006; 316:476–8; author reply 9.
12. Chou TC. Theoretical basis, experimental design, and computerized simulation of synergism and antagonism in drug combination studies. Pharmacol Rev 2006; 58:621–81.
13. Zhou G, Bennett PV, Cutter NC, Sutherland BM. Proton-HZE-particle sequential dual-beam exposures increase anchorage-independent growth frequencies in primary human fibroblasts. Radiat Res 2006; 166:488–94.
14. Boedeker W, Backhaus T. The scientific assessment of combined effects of risk factors: different approaches in experimental biosciences and epidemiology. Eur J Epidemiol 2010; 25:539–46.
15. Brun YF, Greco WR. Characterization of a three-drug nonlinear mixture response model. Front Biosci (Schol Ed) 2010; 2:454–67.
16. Tallarida RJ. Revisiting the isobole and related quantitative methods for assessing drug synergism. J Pharmacol Exp Ther 2012; 342:2–8.
17. Siranart N, Blakely EA, Cheng A, Handa N, Sachs RK. Mixed beam murine harderian gland tumorigenesis: predicted dose-effect relationships if neither synergism nor antagonism occurs. Radiat Res 2016; 186:577–91.
18. Sollazzo A, Shakeri-Manesh S, Fotouhi A, Czub J, Haghdoost S, Wojcik A. Interaction of low and high LET radiation in TK6 cells-mechanistic aspects and significance for radiation protection. J Radiol Prot 2016; 36:721–35.
19. Lam GK. The interaction of radiations of different LET. Phys Med Biol 1987; 32:1291–309.
20. Kim MH, Rusek A, Cucinotta FA. Issues for simulation of galactic cosmic ray exposures for radiobiological research at ground-based accelerators. Front Oncol 2015; 5:122.
21. Norbury JW, Schimmerling W, Slaba TC, Azzam EI, Badavi FF, Baiocco G, et al. Galactic cosmic ray simulation at the NASA Space Radiation Laboratory. Life Sci Space Res (Amst) 2016; 8:38–51.
22. Curtis SB, Townsend LW, Wilson JW, Powers-Risius P, Alpen EL, Fry RJ. Fluence-related risk coefficients using the Harderian gland data as an example. Adv Space Res 1992; 12:407–16.
23. Hanin L, Zaider M. On the probability of cure for heavy-ion radiotherapy. Phys Med Biol 2014; 59:3829–42.
24. Cucinotta FA, Chappell LJ. Non-targeted effects and the dose response for heavy ion tumor induction. Mutat Res 2010; 687:49–53.
25. Cucinotta FA, Kim MH, Chappell LJ. Space radiation cancer risk projections and uncertainties – 2012. Hanover, MD: NASA Center for AeroSpace Information; 2013. (https://go.nasa.gov/2z8Iobs)
26. Hada M, Chappell LJ, Wang M, George KA, Cucinotta FA. Induction of chromosomal aberrations at fluences of less than one HZE particle per cell nucleus. Radiat Res 2014; 182:368–79.
27. Chang PY, Cucinotta FA, Bjornstad KA, Bakke J, Rosen CJ, Du N, et al. Harderian gland tumorigenesis: low-dose and let response. Radiat Res 2016; 185:449–60.
28. Cacao E, Hada M, Saganti PB, George KA, Cucinotta FA. Relative biological effectiveness of HZE particles for chromosomal exchanges and other surrogate cancer risk endpoints. PLoS One 2016; 11:e0153998.
29. Shuryak I. Quantitative modeling of responses to chronic ionizing radiation exposure using targeted and non-targeted effects. PLoS One 2017; 12:e0176476.
30. Cucinotta FA, Cacao E. Non-targeted effects models predict significantly higher Mars mission cancer risk than targeted effects models. Sci Rep 2017; 7:1832.
31. Hatzi VI, Laskaratou DA, Mavragani IV, Nikitaki Z, Mangelis A, Panayiotidis MI, et al. Non-targeted radiation effects in vivo: a critical glance of the future in radiobiology. Cancer Lett 2015; 356:34–42.
32. Brenner DJ, Little JB, Sachs RK. The bystander effect in radiation oncogenesis: II. A quantitative model. Radiat Res 2001; 155:402–8.
33. Matloff N. The art of R programming. San Francisco: No Starch Press; 2011.
34. Cass S, Diakopoulos N, Romero JJ. The top 10 programming languages. IEEE Spectrum's 2014 Ranking. New York: Institute of Electronic Engineers; 2014. (http://bit.ly/1jZ3b8n).
35. Binder K. Introduction: general aspects of computer simulation techniques and their applications in polymer physics. In: Binder K, editor. Monte Carlo and molecular dynamics simulations in polymer science. Oxford: Oxford University Press; 1995.
36. Alpen EL, Powers-Risius P, Curtis SB, DeGuzman R. Tumorigenic potential of high-Z, high-LET charged-particle radiations. Radiat Res 1993; 136:382–91.
37. Katz R. Radiobiological modeling based on track structure. In: Kiefer J, editor. Quantitative mathematical models in radiation biology. Berlin and Heidelberg: Springer-Verlag; 1988. (http://digitalcommons.unl.edu/physicskatz/60)
38. Cucinotta FA, Nikjoo H, Goodhead DT. Applications of amorphous track models in radiation biology. Radiat Environ Biophys 1999; 38:81–92.
39. Goodhead DT. Energy deposition stochastics and track structure: what about the target? Radiat Prot Dosimetry 2006; 122:3–15.
40. Cucinotta FA, Kim MH, Chappell LJ, Huff JL. How safe is safe enough? Radiation risk for a human mission to Mars. PLoS One 2013; 8:e74988.
41. Fry RJ, Powers-Risius P, Alpen EL, Ainsworth EJ. High-LET radiation carcinogenesis. Radiat Res 1985; 8:S188–95.
42. Alpen EL, Powers-Risius P, Curtis SB, DeGuzman R, Fry RJ. Fluence-based relative biological effectiveness for charged particle carcinogenesis in mouse Harderian gland. Adv Space Res 1994; 14:573–81.
43. Cucinotta FA. Review of NASA approach to space radiation risk assessments for Mars exploration. Health Phys 2015; 108:131–42.
44. Brauer F, Nohel J. The qualitative theory of ordinary differential equations. New York: Dover; 1989.
45. Shuryak I, Fornace AJJ Jr, Datta K, Suman S, Kumar S, Sachs RK, et al. Scaling human cancer risks from low LET to high LET when dose-effect relationships are complex. Radiat Res 2017; 187:476–82.